Eur. Phys. J. C (2005)
Digital Object Identifier (DOI) 10.1140/epjc/s2005-02206-1

THE EUROPEAN PHYSICAL JOURNAL C

Low mass dimuon production in proton-nucleus collisions with the NA60 apparatus

The NA60 Collaboration

H.K. Wöhri[2,4,a], R. Arnaldi[8], R. Averbeck[10], K. Banicz[2], J. Buytaert[2], J. Castor[3], B. Chaurand[6], B. Cheynis[3], C. Cicalo[1], P. Cortese[8], A. David[2,4], A. de Falco[1], A. Devaux[3], A. Drees[10], L. Ducroux[5], H. En'yo[7], A. Ferretti[8], M. Floris[1], P. Force[3], J.-Y. Grossiord[5], N. Guettet[2], A. Guichard[5], H. Gulkanian[9], J. Heuser[7], M. Keil[2], L. Kluberg[6], J. Lozano[4], C. Lourenço[2], F. Manso[3], A. Masoni[1], A. Neves[4], H. Ohnishi[7], C. Oppedisano[8], G. Puddu[1], E. Radermacher[2], P. Rosinsky[2], E. Scomparin[8], J. Seixas[4], S. Serci[1], R. Shahoyan[2,4], P. Sonderegger[4], G. Usai[1]

[1] Università di Cagliari and INFN, Cagliari, Italy
[2] CERN, Geneva, Switzerland
[3] LPC, Université Blaise Pascal and CNRS-IN2P3, Clermont-Ferrand, France
[4] IST-CFTP, Lisbon, Portugal
[5] IPN-Lyon, Université Claude Bernard Lyon-I and CNRS-IN2P3, Lyon, France
[6] LLR, Ecole Polytechnique and CNRS-IN2P3, Palaiseau, France
[7] RIKEN, Wako, Saitama, Japan
[8] Università di Torino and INFN, Italy
[9] YerPhI, Yerevan, Armenia
[10] SUNY Stony Brook, New York, USA

Received: 15 February 2005 / Revised version: 25 February 2005 /
Published online: 8 July 2005 –

Abstract. During the June 2002 run NA60 collected around 600 000 dimuon triggers in proton-nucleus collisions at 400 GeV. We show that the collected dimuon mass spectra can be understood in terms of known sources. The specific target setup, consisting of Beryllium, Indium and Lead targets, simultaneously exposed to the beam, allowed us to study the nuclear dependence of the production cross-section of the ω and ϕ resonances. The elementary nucleon-nucleon production cross-sections at 400 GeV for the ρ, ω and ϕ mesons are also presented. By using the η-Dalitz decay, dominating the mass range below 450 MeV, we, furthermore, extracted the η production cross-section and its nuclear dependence. The results are discussed in the framework of previous measurements, mostly obtained in different decay channels, performed by NA27, HELIOS-1 and CERES-TAPS.

PACS. 25.75.Dw, 25.75.Nq

1 Introduction

Considerable efforts are currently being invested in the study of high-energy heavy-ion collisions. The main goals of this experimental program are the discovery of the phase transition from confined hadronic matter to deconfined partonic matter, predicted by Lattice QCD calculations to occur when the system exceeds a given critical threshold in energy density or temperature [1], and the study of the physical properties of the new phase. The proof of existence of this phase and the study of its properties are key issues in the understanding of confinement and of chiral-symmetry. Several observations have already been made, strongly indicating that a new state of matter is produced in heavy-ion collisions at SPS energies [2], but important issues remain unclear in those observations. NA60 was explicitly designed [3] to provide new and more accurate measurements which should clarify specific questions raised by the previous experiments, all of them addressing physics topics accessible through the measurement of dilepton production.

In particular, NA60 wants to clarify if the properties (mass and width) of the ρ resonance are changed by the strongly interacting dense medium created in heavy-ion collisions, as suggested by the observations published by the CERES Collaboration [5]. Such studies much rely on a solid understanding of low mass dilepton production in proton-nucleus collisions, which provide a reference baseline with respect to which the heavy-ion specific phenomena can be extracted.

Moreover, there is some independent physics interest in this mass region for proton-induced interactions, linked

[a] e-mail: hermine.woehri@cern.ch

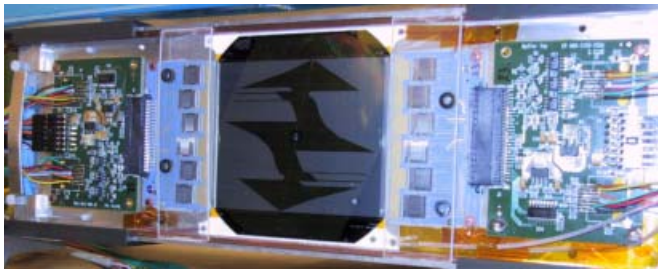

Fig. 1. A silicon microstrip plane with the corresponding front-end electronics. Each sensor has a central hole of 3.6 mm diameter to let the non-interacting beam protons pass through

to the historical puzzle of "anomalous lepton pair" production, which dates back to the mid-seventies and early eighties, when a series of publications, both on e^+e^- and on $\mu^+\mu^-$ pairs, reported an excess of the observed yield above the expectation from meson decays (see [4] and references therein). More recently, HELIOS-1 [4] showed, by direct measurements of certain Dalitz modes, that the yield of e^+e^- and $\mu^+\mu^-$ pairs in 450 GeV p-Be collisions could essentially be accounted for by meson decays, thereby ruling out the existence of such an anomaly. The CERES [6] and NA38/NA50 [7] collaborations also contributed to this story, the latter reporting the observation of a low-mass excess for transverse momentum above 1 GeV/c.

2 Detector setup, data taking and reconstruction

The concept followed by NA60 is to trigger on, identify and reconstruct two muon tracks in a muon spectrometer, inherited from NA50, and to remeasure their momenta and angles with improved accuracy in a Silicon vertex telescope placed just after the target and immersed in a 2.5 T dipole magnetic field. The muon spectrometer consists of a hadron absorber, 4 trigger hodoscopes and two sets of 4 multi-wire proportional chambers (MWPC) placed before and after an air-core toroidal magnet (ACM), operated at ±4000 A. The MWPC's measure the passing particles' coordinates in three independent wire planes, rotated by 60°. The muon identification requires a hit in the last trigger hodoscope, placed after a 1.2 m thick Iron wall at the very end of the apparatus. During the 400 GeV proton run of 2002 the vertex telescope was built from Silicon microstrip sensors, developed and produced at BNL, whose segmentation was adapted to the highly inhomogeneous particle production across the sensor surface so that the occupancy always stayed below 3 %, even in p-Pb interactions [8]. A 4-chip Silicon pixel plane [9] was also used during part of the data taking period. Figure 1 shows one microstrip plane, with the sensor surrounded by the corresponding front-end electronics.

The number of incident protons was measured over the whole data taking period by means of 3 independent ionisation chambers, placed upstream of the target. Typical beam intensities were a few 10^8 protons per burst with a spill length of 4.8 s and a SPS cycle of 16.8 s. The target system consisted of four Beryllium, an Indium and a Lead target, with total respective thicknesses of 2 %, 0.9 % and 1.2 % nuclear interaction lengths. In order to reduce systematic uncertainties in the extraction of the nuclear dependence of the production cross-sections, all targets were *simultaneously* exposed to the beam. The 6 targets were 2 mm thick and had an interspacing of 8 mm. Their diameters, 12 mm, were large enough to fully intercept the proton beam.

The data was reconstructed with the `NA60root` detector simulation and reconstruction package. It starts by reconstructing tracks in the muon spectrometer, discarding already a significant amount of events ($\sim 50\%$), where the trigger pattern was coincidently fired by random hits. Only if at least two muons were reconstructed, and with their origin in the target region, the tracking in the vertex telescope is performed. If at least two tracks in the vertex telescope are found the event reconstruction proceeds to the vertexing step. For the beam intensities used we expect an interaction pile-up rate of $\sim 20\%$. In order to uniquely assign the muons to the target where they were produced, all events where two vertices were reconstructed were discarded. A detailed Monte Carlo study showed that in only $\sim 2\%$ of the generated events the collision vertex was reconstructed in a wrong target. The matching of the muons coming from the muon spectrometer to candidate tracks in the vertex telescope was done by taking into account the multiple scattering and energy loss of the muons in the hadron absorber and was performed in coordinate and momentum space [10]. Since the particle multiplicities in p-A collisions are relatively small, the rate of fake matches is negligible. However, since the vertex telescope's acceptance does not entirely cover the angular acceptance of the muon spectrometer, mostly due to the beam hole in the strip sensors, it can happen that the matching fails, especially for very forward tracks produced in the more downstream targets.

Apart from having collected dimuons of opposite sign, we have also collected like-sign muon pairs in order to estimate the so-called "combinatorial background", mainly consisting of coincidentally paired muons from pion and kaon decays. The evaluation was done through a "mixed event technique", in which single muons (from like-sign pairs) of *different* events are combined to form a muon pair. Only pairs which satisfy the trigger condition were used. This procedure provides the shape of the background contribution; the normalisation was then carefully evaluated respecting the correlations imposed by our trigger.

3 Expected dimuon sources

The dimuon mass spectrum is a rich superposition of various sources resulting in a continuously falling shape, decorated with several pronounced resonances. The continuous processes are the Drell-Yan dimuons, which are dominating at large dimuon masses (above ~ 3.5 GeV) and the semi-muonic simultaneous decays from two (correlated) D mesons. At the lower end of the dimuon mass spectrum

Table 1. Processes simulated with "Genesis" and the branching ratios [13] considered in our study

	Particle	Decay	BR
Dalitz	η	$\mu^+\mu^-\gamma$	$(3.1 \pm 0.4) \cdot 10^{-4}$
	η'	$\mu^+\mu^-\gamma$	$(1.04 \pm 0.26) \cdot 10^{-4}$
	ω	$\mu^+\mu^-\pi^0$	$(9.6 \pm 2.3) \cdot 10^{-5}$
2-body	η	$\mu^+\mu^-$	$(5.8 \pm 0.8) \cdot 10^{-6}$
	ρ	$\mu^+\mu^-$	$(4.55 \pm 0.28) \cdot 10^{-5}$
	ω	$\mu^+\mu^-$	$(7.14 \pm 0.13) \cdot 10^{-5}$
	ϕ	$\mu^+\mu^-$	$(2.85 \pm 0.19) \cdot 10^{-4}$

the electromagnetic decays of the light pseudo-scalar and vector mesons (η, η', ρ, ω and ϕ) are the dominating processes, adding to the continuous spectrum via their Dalitz decays and/or giving rise to distinct peaks via their 2-body decays. While the Drell-Yan and open charm processes were simulated with the Pythia event generator [11], version 6.208, the "hadronic decay cocktail" was generated with "Genesis", as described below. All simulated processes were immersed in an underlying hadronic event, generated with VENUS [12], version 4.12, so that the resulting reconstruction efficiencies are as realistic as possible. These events were then tracked through the NA60 apparatus, using GEANT, version 3.21, with the probability for a generated track to leave a hit in a given microstrip detector plane being proportional to the previously determined strip efficiencies. Events in which a dimuon satisfied the trigger conditions were reconstructed in the same way as the collected data. In this way, we reproduce the effects imposed by the detector, such as the finite acceptance window, the energy loss, and the smearing of the kinematic variables through multiple scattering or due to the finite resolution of the apparatus.

Table 1 lists the particle production processes simulated with "Genesis" together with the respective branching ratios into muons [13]. Note that we have used the electronic branching ratio for the ω 2-body decay, assuming lepton universality, since it is known with much better accuracy than the muonic value.

The kinematical distributions of the light mesons ($p_{\rm T}$ and rapidity) were generated with distributions which describe reasonably well the existing data, mainly collected at the CERN-SPS. The $p_{\rm T}$ distributions were generated according to the functional form $1/p_{\rm T}\,{\rm d}N/{\rm d}p_{\rm T} = m_{\rm T} \cdot K_1(m_{\rm T}/T)$, where K_1 is the modified Bessel function and the "inverse slope" parameter, T, is commonly associated with the effective temperature of the matter created by the collision, at the moment of kinetic freeze-out. The rapidity, y, distributions were generated according to the expression $1/\cosh^2(ay)$, similar to a Gaussian of $\sigma = 0.75/a$. The width of the pion rapidity distribution was estimated using Landau's expression $\sqrt{\log \gamma_{\rm proj}}$ and the width of the rapidity distribution for heavier mesons was decreased proportionally to the maximum rapidity (in the c.m.s. frame, y^*) with which such a meson can be produced, $\sigma_{\rm part} = \sigma_\pi \cdot y^*_{\rm max}(m_{\rm part})/y^*_{\rm max}(m_\pi)$, with $y^*_{\rm max}(m) = \log(\sqrt{s}/m)$.

For the mass line shapes of the narrow resonances η, ω and ϕ, we have used a modified relativistic Breit-Wigner parameterisation, first proposed by G.J. Gounaris and J.J. Sakurai [14], with the widths and masses taken from the Pythia decay tables. Due to its broadness the shape of the ρ is highly influenced by phase space effects and by the production mechanism. With respect to previous parameterisations, its decay width was replaced by a mass dependent width, $\Gamma_\rho(M)$, and momentum dependent terms were introduced [15]. Integrating over the 3-momentum we obtain the following rate equation, from which the ρ was generated:

$$\frac{{\rm d}R(M)}{{\rm d}M} = \frac{\alpha^2 m_\rho^4}{3(2\pi)^4} \frac{\left(1-\frac{4m_\pi^2}{M^2}\right)^{3/2}\sqrt{1-\frac{4m_\mu^2}{M^2}}\left(1+\frac{2m_\mu^2}{M^2}\right)}{(M^2-m_\rho^2)^2 + M^2\Gamma_{\rm tot}^2} \times (2\pi MT)^{3/2} e^{-M/T} \quad .$$

In this equation T is the hadronisation "temperature" parameter, 170 MeV, as deduced from ratios of particle yields in elementary reactions and nuclear collisions at SPS energies [16]. The dimuon mass distributions for muons coming from Dalitz decays were generated according to the Kroll-Wada form [17], multiplied by the electromagnetic transition from factor, $|F(q^2)|^2$. The form factors were taken from a fit to the Lepton-G data [18].

The azimuthal decay angle of the two muons is generated isotropic for all decay modes. For the polar decay angle we have used two possible distributions in the case of the 2-body decays: uniform and $1+\cos^2\theta$. In the Dalitz decays, the two muons are accompanied by a third decay partner, a real photon or a π^0. Due to angular momentum conservation the muons from η and η' Dalitz decays are expected to have a $1+\cos^2\theta$ distribution, while the muons of the ω Dalitz decay are expected not to be emitted under a preferred angle.

The open charm events were simulated using the recent CTEQ6L parton distribution functions [19], a mass of the charm quark of $m_{\rm c} = 1.35$ GeV and a $\langle k_{\rm T}^2 \rangle$ of 0.8 $({\rm GeV}/c)^2$. The muonic branching ratios of the various charmed hadrons were taken from the PDG tables [13]. The absolute cross-section was taken from a compilation of charm measurements [20] and scaled linearly with the mass number, A, apart from the nuclear effects on the parton distribution functions, evaluated with the EKS98 parameterisation [21]. The $c\bar{c}$ cross-sections used were 0.167, 2.25 and 4.14 mb for the p-Be, p-In and p-Pb collision systems, respectively.

The Drell-Yan process was simulated with the "MRS-A Low Q^2" parton distribution functions [22], so that we could generate events down to the lowest possible dimuon mass. Nevertheless, Drell-Yan cannot be calculated for masses lower than 1 GeV. In any case, it is reasonable to assume that such a contribution is negligible with respect to the hadronic decays. Since quark-antiquark annihilation depends on the charge of the interacting quarks and the nucleons have different quark contents, we have generated both types of elementary interactions: pn and

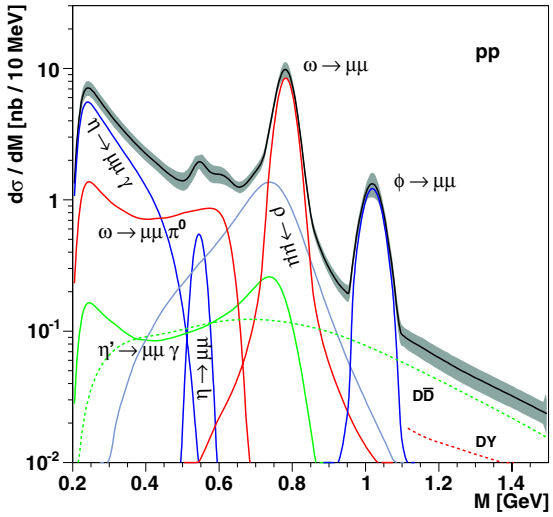

Fig. 2. Generated dimuon mass spectrum for pp collisions at 400 GeV, including smearing

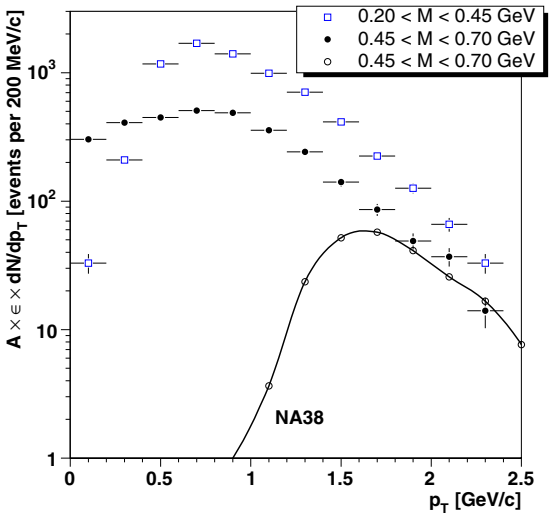

Fig. 3. Measured p_{T} distributions for two mass windows, compared to NA38's distribution of its lowest mass window

pp. Drell-Yan dimuons, also being produced in "hard interactions", are known to scale linearly with the number of nucleons in the nucleus, $\sigma_{\mathrm{pA}} = \sigma_{\mathrm{pp}} \cdot \mathrm{Z} + \sigma_{\mathrm{pn}} \cdot (\mathrm{A} - \mathrm{Z})$, A being the mass number and Z the atomic number. The pn and pp cross-sections were obtained from a comparison [23] of Pythia calculations with DY data from the NA3 Collaboration, collected in p-Pt collisions at 400 GeV [24], $\sigma_{\mathrm{pp}}^{\mathrm{DY}} = 16.7$ nb and $\sigma_{\mathrm{pn}}^{\mathrm{DY}} = 14.7$ nb.

In Fig. 2 we can see the dimuon mass spectrum generated with the hadronic decay cocktail, open charm and Drell-Yan, in pp collisions, smeared with the mass resolution measured at the ω and ϕ resonances. For the purpose of this illustration, we normalised the hadronic decay sources following the procedure outlined in [7].

4 Acceptances and phase space window

Like most experiments, the NA60 detector does not have 4π coverage. The aperture of the ACM magnet, in particular, determines the angular coverage of the muon spectrometer, which can be translated into an acceptance window in dimuon rapidity. The existence of the hadron absorber, on the other hand, imposes a minimum threshold on the energy of the measured muons. Furthermore, the beam hole of the Silicon sensors reduces the angular coverage of the (low p_{T}) muons produced in the most downstream targets. For the extraction of the nuclear dependence of the ω and ϕ mesons, we cannot compare the forward rapidity ϕ mesons produced in the most upstream target (Indium) with the backward rapidity ϕ mesons produced in the last Beryllium target. For this reason, we apply a cut on the (single) muon's angle, or pseudo-rapidity, η. On the other hand, the presence of the vertex magnet largely increases the acceptance for opposite sign low mass and low p_{T} dimuons. Such dimuons would be lost in the dead area around the beam line, if it were not for the vertex magnet which deflects them into the angular acceptance of the muon spectrometer. In Fig. 3 we compare the raw data p_{T} distribution for two different mass windows to the lowest mass window seen by the predecessor experiment NA38. For masses above 400 MeV we have good acceptance down to zero p_{T}, and for masses down to threshold we have good acceptance for p_{T} larger than ~ 400 MeV/c. Since the p_{T} acceptance for low mass dimuons depends also on rapidity, we included a rapidity dependent m_{T} cut in the definition of our phase space window: $3.3 < y_{\mathrm{lab}}^{\mu\mu} < 4.2$, $|\cos\theta_{\mathrm{CS}}| < 0.5$, $\eta_{\mu} < 4.2$, $m_{\mathrm{T}} > 0.7 \cdot (y_{\mathrm{lab}} - 4.2)^2 + 0.4$ GeV, where θ_{CS} is the Collins-Soper angle. In this window the ω and ϕ mesons have acceptances in the ranges 3.2–4.0 % and 6.1–7.2 %, respectively, depending on the z position where they were produced. Their differential acceptances do not vary by more than a factor 10 between any two selected events.

5 Results on low mass dimuon production

Through the muon track matching we have achieved important improvements in the dimuon mass resolution and in the signal to background ratio, which can be appreciated in Fig. 4. Through the matching the background level drops from ~ 30 % to 10 %. After the matching the ω and ϕ are measured with 30 MeV mass resolution. It is worth noting that our Monte Carlo simulations reproduce the measured dimuon mass resolutions. In the right panel of Fig. 4 we can see the dimuon mass distribution in a linear scale, showing a hint of the η peak. After muon track matching and having applied the vertex selection and phase space cuts, the final event sample consists of around 15 000 opposite sign dimuon events.

In order to evaluate the nuclear dependence of the production cross-sections for the η, ω and ϕ resonances we use a power law parameterisation, $\sigma_{\mathrm{pA}} = \sigma_0 \cdot \mathrm{A}^{\alpha}$, where A is the mass number of the target nucleus and σ_0 can be interpreted as the "elementary nucleon-nucleon production cross-section". The values of σ_{pA}, for each process and

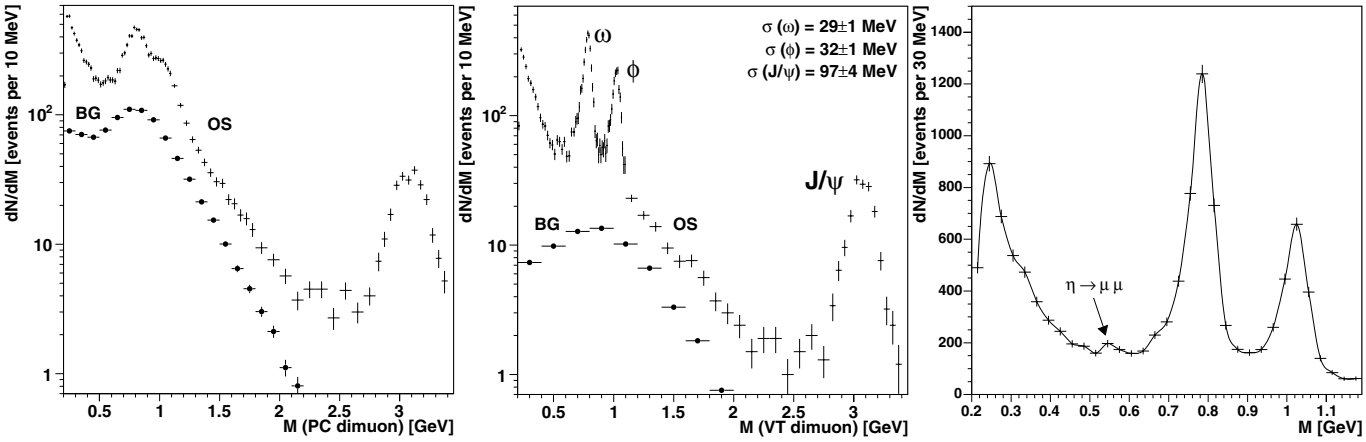

Fig. 4. Opposite sign (OS) and combinatorial background (BG) dimuon mass distributions before (left) and after (centre) muon track matching (sum of all targets). Right: Low mass dimuons in a linear scale

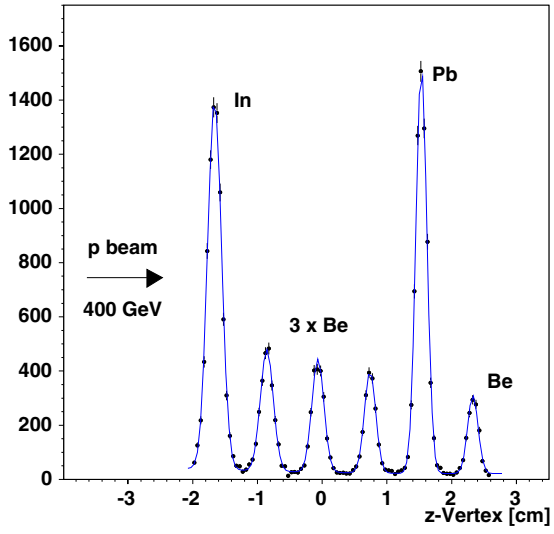

Fig. 5. z-vertex distribution

in each target, are obtained by fitting the measured data to a superposition of the reconstructed Monte Carlo histograms, properly normalised to account for the integrated luminosity, the branching ratios, the acceptances and the efficiencies. The value of α is derived by simultaneously studying the dimuon mass distributions measured in the Be, In and Pb targets. In Fig. 5 we can see the z-vertex distribution for the selected events, showing that the interaction vertex can be uniquely assigned to the individual subtargets.

We use acceptances calculated with respect to the full phase space. This implies assuming generation functions, in y, $\cos\theta$, etc., outside the phase space window where we cannot check their validity. Since there is little knowledge on the distribution of the decay angle θ, we will use both, $1 + \cos^2\theta$ and uniform distributions, when quoting our results.

The opposite-sign dimuon mass distributions obtained from the p-Be, p-In and p-Pb data samples, taking together the satistics of all Beryllium targets, are *simultaneously* fitted to a superposition of all the expected sources. The combinatorial background, open charm and Drell-Yan contributions are fixed as outlined above and describe the mass region above 1.2 GeV very well in *all* three data samples. The fit, carried out in the mass range 0.2–1.1 GeV includes 7 free parameters: the σ_0 and α values of the η, ρ, ω and ϕ contributions, imposing the same α for the ρ and ω mesons. The η' is assumed to be produced proportionally to the η, $\sigma^{\eta'} = 0.15 \cdot \sigma^{\eta}$ [6]. The result of the fit is shown in Fig. 6 for the three target materials. The fitted contributions of the 2-body and Dalitz decays are drawn on top of the sum of the combinatorial background, open charm and Drell-Yan processes, shown as the lowest solid line. The data points are very well described by the sum of the expected contributions, with the elementary full phase space cross-sections and α values listed in Table 2. The quoted errors refer to statistical uncertainties only. From the fit we can also derive the number of ω's and ϕ's present in our final data samples: $N^{\omega} = 966$, 676 and 660, $N^{\phi} = 575$, 464 and 511, for the Be, In and Pb targets, respectively.

Table 2. Elementary full phase space production cross-sections, and their dependences on the mass number A, for the η, ρ, ω and ϕ mesons, as extracted from a simultaneous fit to the three dimuon mass spectra

	$1 + \cos^2\theta$	uniform
σ_0^{η} [mb]	9.5 ± 0.6	10.2 ± 0.6
σ_0^{ρ} [mb]	11.6 ± 1.0	8.9 ± 0.7
σ_0^{ω} [mb]	10.5 ± 0.6	8.0 ± 0.5
σ_0^{ϕ} [mb]	0.53 ± 0.05	0.40 ± 0.03
α^{η}	0.93 ± 0.02	
α^{ω}	0.82 ± 0.01	
α^{ϕ}	0.91 ± 0.02	

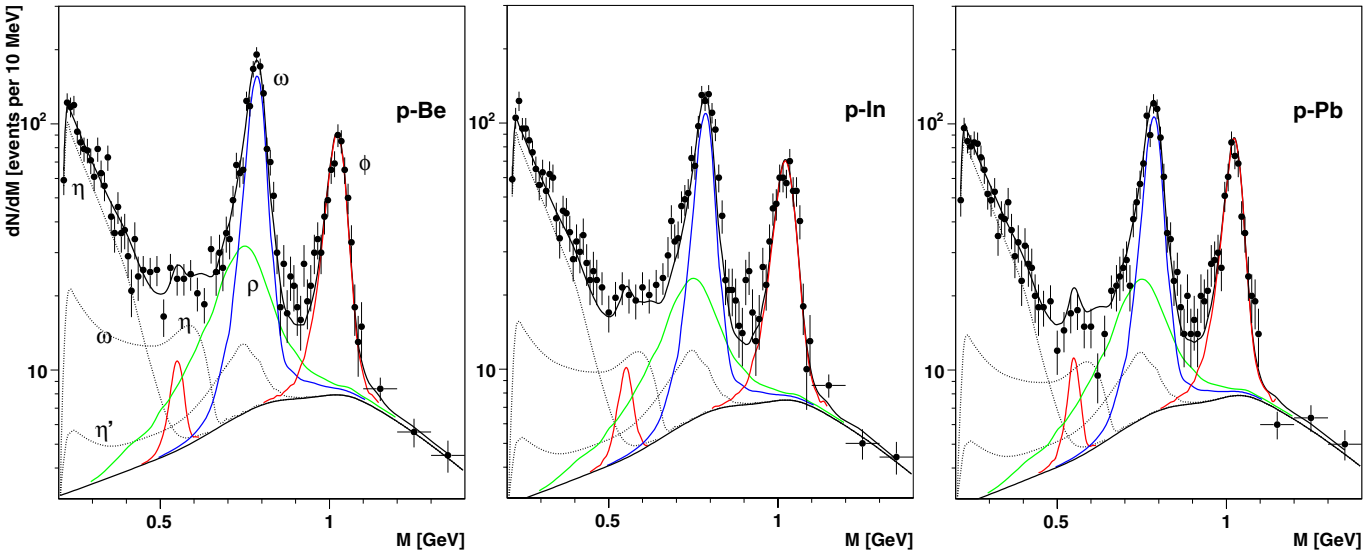

Fig. 6. Fit to the dimuon mass spectra collected in p-Be, p-In and p-Pb interactions

6 Discussion and conclusions

We have presented the nuclear dependence of the η, ω and ϕ production cross-sections, expressed by the α values. We see the ϕ production cross-section increasing with the target's mass number significantly faster than the ω, an observation relevant for the interpretation of the "ϕ enhancement" observed in heavy-ion collisions by NA38 and NA50 [25]. Also the η has a higher α value, with respect to the ω. However, since the acceptance of the NA60 detector steeply drops for low $p_{\rm T}$ dimuons of low masses (below $M \sim 400$ MeV) and the η's fit parameters are mainly fixed from its Dalitz decay, most of the η's in our event sample have larger $p_{\rm T}$ values than the dimuons resulting from ω and ϕ decays. It is well known that α increases with $p_{\rm T}$ ("Cronin effect"). Hence, if we want to compare the α of the η to that of the ω and ϕ we have to take into account the $p_{\rm T}$ dependence, a point presently under investigation.

The second result of the present study is the elementary (nucleon-nucleon) production cross-sections for the η, ρ, ω and ϕ mesons at 400 GeV. NA27 also published full phase space particle production cross-sections at exactly the same energy [26]. Measuring the four mesons in hadronic and electromagnetic decays, they obtained the following values: $\sigma^{\eta} = 9.8 \pm 0.6$, $\sigma^{\rho} = 12.6 \pm 0.6$, $\sigma^{\omega} = 12.8 \pm 0.8$ and $\sigma^{\phi} = 0.62 \pm 0.06$ mb. Before we compare the NA27 values to our own measurements it is important to note that, given their similar masses, the ρ and ω mesons are affected by interference effects when measured in the same decay channel. A detailed study was performed by the HELIOS-1 experiment [4], which found a negative interference effect, leading to a measured "$\sigma^{\rho/\omega}$" total production cross-section in the dilepton decay channel 15 % smaller than the sum of the individual production cross-sections, $\sigma^{\rho} + \sigma^{\omega}$, as measured in independent decay channels. Assuming that our dimuon data is affected by the same interference effect as derived by HELIOS-1, we deduce a total $\rho + \omega$ production cross-section, corrected for the interference effect, of $\sigma^{\rho} + \sigma^{\omega} = 25.4 \pm 1.3$ mb in remarkable agreement with the NA27 value, 25.4 ± 1.0 mb. There is also a perfect agreement between the two experiments in what concerns the η resonance. Our ϕ value is ~ 20 % lower than the one quoted by NA27. It should be noted, however, that the value derived by NA27 seems to be somewhat overestimated, judging from the measurements shown in their publication. This comparison was done using the values we obtained with the $1 + \cos^2\theta$ decay angle distributions. If we would use those corresponding to uniform $\cos\theta$ distributions the agreement with NA27 would considerably degrade, an indication that the $1 + \cos^2\theta$ distributions provide a better description of the ρ, ω and ϕ dimuon decays.

We can also compare our results with the HELIOS-1 and CERES-TAPS measurements. HELIOS-1, measuring dielectrons *and* dimuons in p-Be collisions at 450 GeV [4], had the capability to fully reconstruct the Dalitz decays. HELIOS-1 also used a $1 + \cos^2\theta$ decay angle distribution to extrapolate their ρ and ω measurements to full phase space, obtaining $\sigma^{\eta}/(\sigma^{\rho}+\sigma^{\omega}) = 0.54 \pm 0.05$ from the e^+e^- data and 0.52 ± 0.06 from the $\mu^+\mu^-$ data, before any correction for interference effects. It should be noted that the η cross-section measured in the $l^+l^-\gamma$ mode provided an excellent description of the *dilepton* mass spectra. Taking the α^{η} and $\alpha^{\omega} = \alpha^{\rho}$ we have measured, we can derive the HELIOS1 nucleon-nucleon values from their p-Be data, measured in a similar kinematics window, obtaining $\sigma_0^{\eta}/(\sigma_0^{\rho} + \sigma_0^{\omega}) = 0.42 \pm 0.04$ for the e^+e^- data and 0.41 ± 0.05 for the $\mu^+\mu^-$ data. These values are in excellent agreement with our result, $\sigma_0^{\eta}/(\sigma_0^{\rho}+\sigma_0^{\omega}) = 0.43 \pm 0.04$. Note that this comparison is not sensitive to the ρ/ω interference. For further comparisons, however, we should correct these values for the interference effect. The NA60 value then becomes 0.37 ± 0.03 while the HELIOS-1 values become 0.37 ± 0.04 (e^+e^-) and 0.35 ± 0.04 ($\mu^+\mu^-$).

Figure 7 compares the $\sigma_0^{\eta}/(\sigma_0^{\rho} + \sigma_0^{\omega})$ value extracted from our data, corrected for ρ/ω interference, with the val-

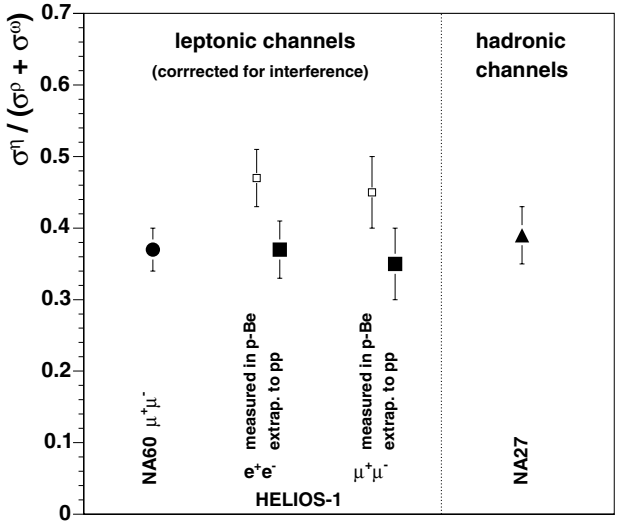

Fig. 7. Comparison between the $\sigma^\eta/(\sigma^\rho + \sigma^\omega)$ value deduced from our data and those of previous experiments, made in leptonic and hadronic decay channels

ues of the other experiments. We conclude that the η yield which best describes our low mass dimuon data is in very good agreement with the measurements of these previous experiments and we do not see the need for additional sources to explain our low mass dimuon data.

Also the CERES-TAPS experiment measured a similar (but not identical) quantity, $\sigma^\eta/(2 \cdot \sigma^\omega)$, in p-Be and p-Au collisions with 450 GeV protons [27]. The values given within their phase space window of $3.1 < y < 3.7$ were 0.34 ± 0.03 and 0.37 ± 0.04 for p-Be and p-Au, respectively. If we extrapolate these measurements to full phase space and to elementary nucleon-nucleon collisions, we obtain 0.31 ± 0.03 from p-Be and 0.24 ± 0.03 from p-Au.

The results presented in this paper will be improved and extended in the near future, thanks to the much higher statistics collected by NA60 in 2004, with 400 GeV protons incident on an expanded target system.

Acknowledgements. We thank the many people who contributed to the feasibility of the measurements analyzed in this paper. The full list is too big to be included here, but we would like to mention explicitly the following names: G. Anelli, F. Bal, A. Boccardi, L. Casagrande, E. Chesi, B. Cheynis, E. David, J. Fargeix, W. Flegel, L. Gatignon, V. Granata, F. Hahn, S. Haider, B. Herskind, P. Jarron, L. Kottelat, D. Marras, P. Martins, I. McGill, H. Muller, T. Niinikoski, R. Oliveira, A. Onnela, V. Palmieri, S. Popescu, P. Ramalhete, J.M. Rieubland, J. Rochez, S. Roe, P. Weilhammer, and H. Vardanyan. The silicon microstrip sensors used in our Beam Tracker and Vertex Telescope were developed and produced at BNL, by W. Chen and Z. Li. The read-out electronics chain of the Beam Tracker was built at LHEP, Bern, by K. Borer. We also acknowledge useful discussions with S. Damjanovic, H. Specht and R. Veenhof. This work was partially supported by the Fundação para a Ciência e Tecnologia, Portugal.

References

1. F. Karsch, Lattice QCD at high temperature and density, Lecture Notes in Physics **583**, 209 (2002)
2. U. Heinz, M. Jacobs, nucl-th/0002042
3. NA60 Proposal, CERN/SPSC 2000-010, and references therein
4. T. Akesson et al. (HELIOS-1 Coll.), Z. Phys. C **68**, 47 (1995)
5. G. Agakichiev et al. (CERES Coll.), Phys. Rev. Lett. **75**, 1272 (1995); Phys. Lett. B **422**, 405 (1998); D. Adamova et al. (CERES Coll.), Phys. Rev. Lett. **91**, 042301 (2003)
6. G. Agakichiev et al. (CERES Coll.), Eur. Phys. J. C **4**, 231 (1998)
7. M.C. Abreu et al. (NA38 and NA50 Coll.), Eur. Phys. J. C **13**, 69 (2000)
8. H.K. Wöhri, PhD thesis, TU Wien, Austria, 2004
9. K. Banicz et al., Nucl. Instrum. Meth. A **539**, 137 (2005)
10. R. Shahoyan et al. (NA60 Coll.), Eur. Phys. J. C **43** (2005)
11. T. Sjöstrand et al., Comp. Phys. Comm. **135**, 238 (2001)
12. K. Werner, Phys. Rep. **232**, 87 (1993)
13. S. Eidelman et al. (PDG), Phys. Lett. B **592**, 1 (2004)
14. G.J. Gounaris, J.J. Sakurai, Phys. Rev. Lett. **21**, 244 (1968)
15. J. Knoll, B. Friman, private communication
16. F. Becattini et al., Phys. Rev. C **69**, 024905 (2004)
17. N.M. Kroll, W. Wada, Phys. Rev. **98**, 1355 (1955)
18. L.G. Landsberg, Phys. Rep. **128**, 301 (1985)
19. J. Pumplin et al., JHEP **0207**, 012 (2002) hep-ph/0201195
20. H. Wöhri, C. Lourenço, J. Phys. G **30**, S315 (2004)
21. K.J. Eskola et al., Eur. Phys. J. C **9**, 61 (1999)
22. A.D. Martin et al., Phys. Rev. D **51**, 4756 (1995)
23. C. Lourenço, PhD thesis, IST, Lisbon, Portugal, 1995
24. J. Badier et al. (NA3 Coll.), Phys. Lett. **89B**, 145 (1979)
25. B. Alessandro et al. (NA50 Coll.), Phys. Lett. B **555**, 147 (2003); Phys. Lett. B **561**, 294 (2003)
26. M. Aguilar-Benitez et al. (NA27 Coll.), Z. Phys. C **50**, 405 (1991)
27. G. Agakichiev et al. (CERES-TAPS Coll.), Eur. Phys. J. C **4**, 249 (1998)